Effects of isotopic composition on the lattice dynamics of CuCl

Andreas Göbel, Tobias Ruf, Cheng-Tian Lin, and Manuel Cardona
Max-Planck-Institut für Festkörperforschung, Heisenbergstr. 1, D-70569 Stuttgart, Germany

Jean-Claude Merle and Marguerite Joucla
Institut de Physique et Chimie des Matériaux, 23 rue du Loess, F-67037 Strasbourg, France
(Received 16 January 1997)

We have investigated the changes in the Raman spectra of CuCl resulting from isotope substitution. Our samples were made from the stable isotopes ^{63}Cu, ^{65}Cu, ^{35}Cl, and ^{37}Cl as well as the natural elements. While the longitudinal-optic (LO) mode shifts according to the expected reduced mass behavior of a Γ-point phonon, the transverse-optic (TO) vibration shows pronounced deviations. Due to the strong anharmonicity of CuCl, the TO mode interacts with a two-phonon combination band of acoustic phonons and one obtains coupled excitations which have been attributed to a Fermi resonance. We describe this process using a shell model for the lattice dynamics of CuCl and only one cubic coefficient for the anharmonic interaction. The Fermi resonance results in an anomalous line shape of the TO phonon, which reflects properties of the zone center mode as well as of the two-phonon combination band. Isotope substitution allows us to discern the two contributions and to check the validity of the model. The off-center model proposed earlier to explain the TO anomaly cannot account for our findings. [S0163-1829(97)07825-9]

I. INTRODUCTION

During the past decade there has been considerable interest in the effects of isotopic composition on the bulk properties of semiconductors. So far, the investigations have largely been confined to group-IV semiconductors.[1–4] In these monoatomic lattices the mass dependence of the phonon frequencies in the harmonic approximation ($\omega \sim 1/\sqrt{m}$) is trivial; i.e., it does not change with the phonon wave vector $\vec{q}$. This facilitates the ability to discern the influence of isotopic disorder on the phonon frequencies, line shapes, and widths from anharmonic contributions.[1] Another bulk property depending on the isotopic composition is the lattice constant at $T=0$ K which is affected by the amplitude of the zero-point motion of the atoms. Since heavier isotopes probe a smaller fraction of the anharmonic lattice potential, one expects a smaller lattice constant when the heavier isotope is enriched with respect to its natural abundance. This was observed by Buschert *et al.*[5] in the case of germanium. Altering the mean-squared atomic displacements in a subtle, well-defined manner, isotope substitution also allows a detailed investigation of the electron-phonon coupling and the renormalization of the band gap.[1–3,6,7]

Recently, we have extended our investigations of isotope effects to compound semiconductors. In contrast to elemental semiconductors, the changes in phonon frequencies and atomic displacements in compounds strongly depend on the phonon branch and wave vector $\vec{q}$, when atoms of the compound constituents are isotopically substituted. Since the acoustic and optic branches of the phonon dispersion are affected differently by the substitution of heavy or light atoms, their energies can be tuned almost independently, in particular at the X point. This allows one to probe the efficiency of the anharmonic decay of Γ-point optical phonons into lower-lying acoustic bands. Similar to elemental semiconductors, the dependence of the lattice constant on the isotopic composition and changes of the fundamental gap due to the electron-phonon coupling have been predicted for zinc-blende semiconductors employing empirical lattice dynamical models and electron pseudopotentials. In the case of GaAs the changes in the gap with the Ga masses are in good agreement with the experimental observation.[8] First principles calculations of the effect of isotope mass on the lattice constant in zinc-blende semiconductors have also been performed.[9]

Copper chloride is among the most ionic semiconductors which crystallize in the zinc-blende structure.[10,11] Being close to phase transitions, its physical properties exhibit a number of peculiarities which have been studied extensively; e.g., the strongly negative linear expansion coefficient at low temperatures[12] and the decreasing elastic shear constants with increasing hydrostatic pressure[13] have been associated with a strongly anharmonic lattice potential. The sizable increase of the direct gap with increasing temperature[14] is anomalous, and changes in the band gap with isotope substitution reveal that the admixture of the copper d electrons to the chlorine p levels is crucial for the structure of the valence band.[8,15–18]

Another prominent feature of CuCl is its anomalous Raman spectrum even at low temperature (2 K). Besides a unanimously accepted LO phonon ($\sim 209\ \mathrm{cm}^{-1}$) it exhibits a broad structure with at least two peaks ($145–175\ \mathrm{cm}^{-1}$) in the TO region,[19–22] instead of the single TO phonon predicted by group theory for zinc-blende compounds. This anomaly does not only occur at the zone center. By means of inelastic neutron scattering it was shown to extend into the Brillouin zone.[23,24] Two interpretations of this anomaly have been offered: On the one hand, Krauzman *et al.* modeled the anomalous TO spectrum of CuCl by a Fermi resonance in which the optical phonon is repelled out of a two-phonon combination band.[21] They followed a procedure outlined ear-

lier by Ruvalds and Zawadowski to calculate the hybridization of a two-phonon resonance with single-phonon states due to third- and fourth-order anharmonic couplings.[25] Subsequent detailed lattice dynamical calculations by Kanellis, Kress, and Bilz showed that third-order anharmonic coupling is sufficient to account for both peaks of the TO phonon structure.[26] On the other hand, a model in which a substantial fraction of the Cu atoms are located at nonideal sites, giving rise to additional vibrational modes, has also been proposed.[27,28] In this model the large anharmonicity is held responsible for secondary minima in the lattice potential, which give rise to Cu displacements from the standard zinc-blende sites.

Recently, this off-center model has been cited in order to support the results of first principles calculations on structural anomalies in the Cu halides. Using all-electron density functional theory, Wei, Zhang, and Zunger obtain a local minimum in the total energy of a 16-atom CuCl supercell, when the copper atom is displaced along the [111] antibonding direction.[29] For a larger supercell, Park and Chadi have found that the total energy of CuCl is lowered even further by the formation of a complex of four Cu off-center atoms.[30] They imply that these complexes could result in local modes and associate them with the anomalous TO phonon spectrum.

In this paper we show that the intricate changes in the Raman spectra obtained from CuCl samples of modified isotopic composition can be explained quantitatively within the framework of the Fermi resonance scenario.[21,22,26] The line shifts, changes in linewidths, and changes in intensity ratios with isotope substitution are compared in detail: It is not necessary to invoke a second set of optical phonons to explain the TO structure.[31–33] The predictions of the off-center model[27] are in qualitative disagreement with our observations.

In Sec. II we discuss the experimental details, while Sec. III presents the data. Section IV introduces the basic concepts of the anharmonic interaction model as well as the specific approximations we have made. Our observations are compared to the Fermi resonance model and the off-center model is also discussed.

II. EXPERIMENTAL DETAILS

Natural copper and chlorine have two stable isotopes each (^{63}Cu: 69.2%, ^{65}Cu: 30.8%, ^{35}Cl: 75.8%, and ^{37}Cl: 24.2%). The elements used to grow our samples were isotopically pure (99.9%) except for the enriched ^{37}Cl which contained about 11% of ^{35}Cl, as determined by mass spectroscopy. In order to avoid trivial effects due to varying chemical impurities and crystalline quality we investigated samples from independent sources and confirmed that the Raman spectra for identical isotopic compositions coincide. The samples are usually platelets of up to 10 mm^2 surface area and a thickness of less than 0.1 mm. Using x-ray diffraction we determined the surface to have the [111] orientation. Most samples were grown by heating Cu metal with the desired isotopic composition in flowing HCl gas. For the samples made from isotopically pure HCl purification of the initial reaction products was achieved by two successive sublimations under vacuum and a zone-melting process. Then a transport method in a closed tube containing H_2 was used to grow platelets. Further details of the sample growth technique have been described elsewhere.[36]

Raman spectra were excited using 1–10 mW of the 4067 Å line of a Kr-ion laser. Other laser lines (5145 Å, 6471 Å) have been used to check for line shape distortions or shifts due to resonance effects.[31] The scattered light was dispersed by a Spex 1404 double monochromator ($f=0.85$ m). Using single-photon counting, the spectra were recorded in backscattering geometry from a [111] surface. The samples were cooled to 1.8–2 K by immersing them in superfluid helium, and special care was taken to keep the sample heating at a minimum. The spectra were calibrated against nearby laser plasma lines.

III. RESULTS

When different atoms in the unit cell are isotopically substituted the changes in the phonon frequencies strongly depend on the eigenvectors. Isotope substitution thus allows one to determine mode eigenvectors as shown recently by Zhang *et al.* for the two coupled E_2 phonons in wurtzite CdS.[37] In the harmonic approximation the optical zone center phonon frequencies of zinc-blende compounds are proportional to the inverse square root of the reduced mass ($\omega\sim 1/\sqrt{\mu}, \mu^{-1}=m_{\text{cation}}^{-1}+m_{\text{anion}}^{-1}$). For convenience, we list the reduced masses of our samples in Table I together with the reduced mass variance parameter g_μ, which characterizes the isotopic reduced mass fluctuations in the sample, and is given by

$$g_\mu=\sum c_i \sum a_j \left[\frac{\overline{\mu}-\mu_{ij}}{\overline{\mu}}\right]^2 .$$

Here c_i and a_j are the concentrations of the cation isotope i and the anion isotope j, respectively. The reduced mass of the compound is $\overline{\mu}$ and the reduced mass due to a particular concentration of cation and anion isotopes is denoted by μ_{ij}. These mass fluctuations soften the $\vec{q}$ conservation rule and give rise to elastic, disorder-induced scattering of phonons.[38] The effect vanishes in isotopically pure samples. Since we are interested in the disorder effect on zone center optic modes, we used the reduced mass to calculate the mass variance parameter. In general the mass variance parameter g depends on the eigenvector of the respective mode and thus on the phonon wave vector $\vec{q}$. In the following we label the peaks in the Raman spectrum with the notation introduced in Ref. 20.

A. LO(γ) phonon

Figure 1 shows the LO(γ) Raman spectra of isotopically modified CuCl. The reduced mass μ of the samples increases from the bottom to the top spectrum. Accordingly, the LO(γ) phonon frequency (~ 209 cm^{-1}) decreases from the bottom to the top. The peak intensities are normalized to 1.

The LO(γ) frequency as a function of the reduced mass is shown in Fig. 2. The error bars indicate the mean square deviation as determined from several measurements on the respective sample. The dashed line corresponds to the reduced mass behavior with respect to the experimental fre-

TABLE I. Reduced mass μ, mass variance g_μ, LO(γ), TO(γ), and TO(β) Raman frequencies and linewidths $\Gamma_{\mathrm{LO}(\gamma)}$ (FWHM) of several isotopically modified CuCl samples at $T=2$ K in units of [cm^{-1}]. The linewidth is corrected for the spectrometer resolution. The errors are the mean square deviation of several measurements.

Sample	μ [amu]	g_μ [10^{-5}]	$\omega_{\mathrm{LO}(\gamma)}$	$\Gamma_{\mathrm{LO}(\gamma)}$	$\omega_{\mathrm{TO}(\gamma)}$	$\omega_{\mathrm{TO}(\beta)}$
$^{63}Cu^{35}Cl$ [a]	22.478	0	210.74(20)	1.65(10)	174.54(20)	156.9(2)
$^{nat}Cu^{35}Cl$	22.556	2.6	210.11(20)	1.34(06)	173.75(10)	156.7(1)
$^{63}Cu^{nat}Cl$	22.677	23.6	209.89(12)	1.75(02)	174.33(07)	156.3(3)
$^{65}Cu^{35}Cl$ [a]	22.728	0	209.50(20)	1.64(10)	172.34(20)	155.7(2)
$^{nat}Cu^{nat}Cl$	22.757	26.4	209.66(23)	1.74(05)	173.52(09)	155.9(2)
$^{65}Cu^{nat}Cl$	22.931	24.1	208.62(23)	1.66(02)	172.05(14)	155.4(3)
$^{nat}Cu^{37}Cl$ [b]	23.285	14.5	207.14(20)	1.48(05)	173.23(15)	155.0(3)

[a]Data were taken at $T=8$K; samples have different orientation and were grown by a different process (Ref. 36).

[b]The ^{37}Cl compound contains about 11% ^{35}Cl.

quency of the natural compound. The agreement with the prediction for an optical Γ-point phonon is excellent. Experimental LO(γ) frequencies for some of the compounds are listed together with the full phonon linewidth at half maximum (FWHM) $\Gamma_{\mathrm{LO}(\gamma)}$ in Table I. The spectrometer resolution can be approximated by a Gaussian of 0.45 cm^{-1} width. We have determined $\Gamma_{\mathrm{LO}(\gamma)}$ by fitting the spectra to a Voigt profile, implicitly assuming a Lorentzian line shape for LO(γ).[39]

B. TO phonon structure

The TO structure has two main features: a very narrow line at $\sim 173\ \mathrm{cm}^{-1}$, usually denoted as TO($\gamma$), and a broad maximum around $\sim 155.5\ \mathrm{cm}^{-1}$, labeled TO($\beta$). Raman spectra of the TO structure are shown in Fig. 3. The spectra are normalized with respect to the TO(γ) peak and where taken during the same scan as the LO(γ) spectra in Fig. 1. Note that we have displayed the spectra in a different order as compared to Fig. 1. The vertical bars indicate the position of TO(β) as determined by averaging the results of several measurements and as given in Table I. The Raman shifts of TO(γ) vs the copper mass of the respective compound are shown in Fig. 4. TO(γ) shifts by $(2.3\pm0.2)\ \mathrm{cm}^{-1}$ when in the samples containing natural chlorine ^{65}Cu is replaced by ^{63}Cu, i.e., much more than the shift of 1.0 cm^{-1} expected from the corresponding change in the reduced mass. Samples of the same copper mass have similar TO(γ) frequencies and

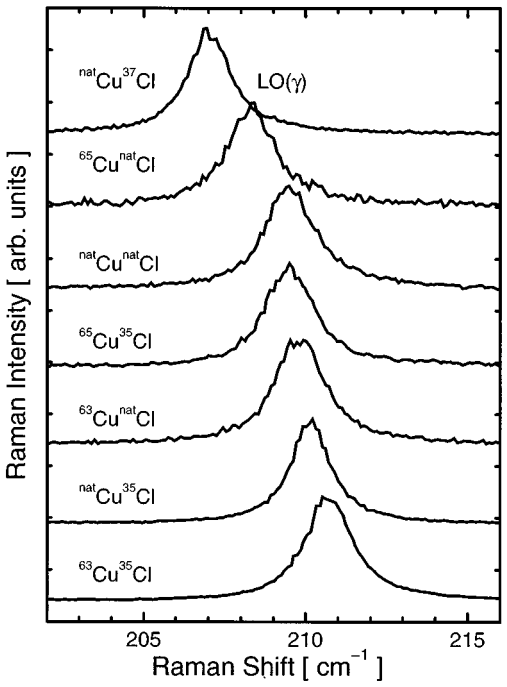

FIG. 1. Raman spectra of the LO phonon of isotopically modified CuCl at 2 K. The reduced mass μ increases from the bottom to the top; LO(γ) shifts according to $\mu^{-1/2}$ as expected for a zone center phonon.

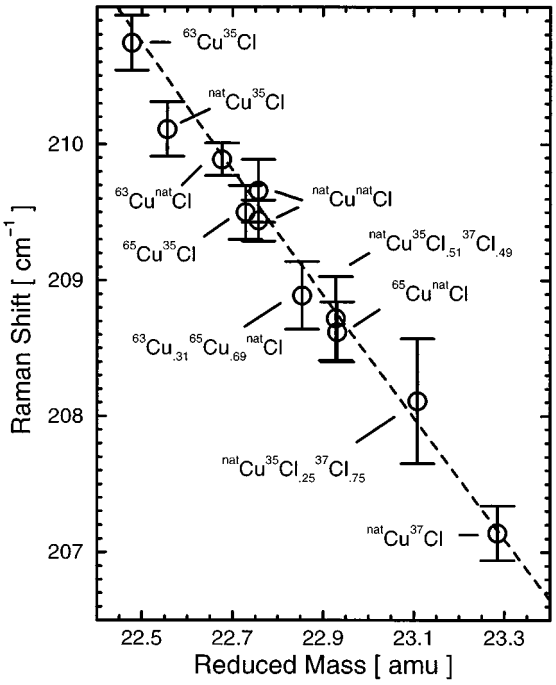

FIG. 2. Raman frequencies of the LO(γ) phonon at $T=2$ K. The data correspond to the samples listed in Table I and others with some additional isotope mixtures. The two data points for natural CuCl stem from samples of independent origin. The solid line represents a reduced mass behavior $\sim\mu^{-1/2}$.

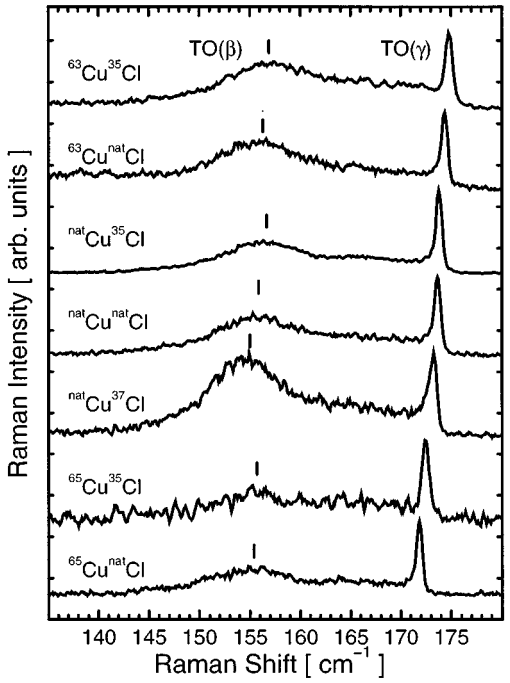

FIG. 3. Raman spectra of the anomalous TO structure for several isotopically modified CuCl samples. The spectra of samples with the same copper mass are grouped together. Within these groups the reduced mass μ decreases from the bottom to the top. The TO(γ) line does not shift according to changes in μ but with changes of the copper mass. The broad TO(β) line shifts according to changes in μ.

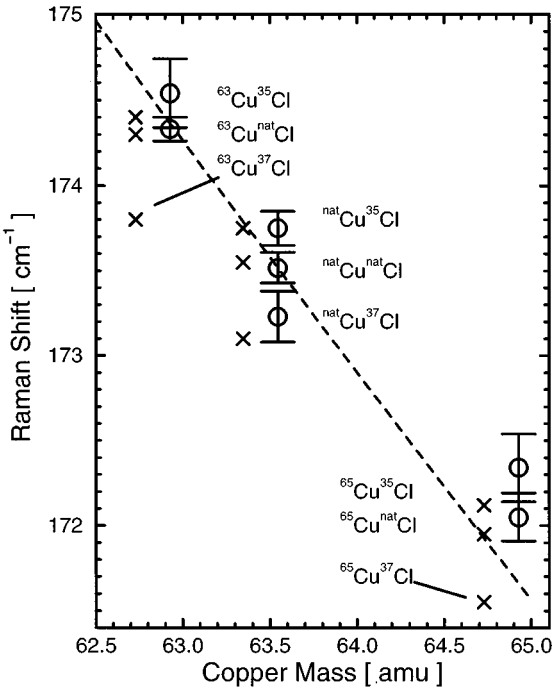

FIG. 4. Raman frequencies of the TO(γ) peak as a function of the copper mass ($T=2$ K, dashed line $\sim m_{Cu}^{-1/2}$ scaled to the frequency in $^{nat}Cu^{nat}Cl$). ○, measured values; ×, calculated values as discussed in Sec. IV C. For clarity, the theoretical values have been shifted by -0.2 amu. The error bars represent the mean square deviation of several measurements.

the shifts observed for chlorine substitution are much smaller than expected from their respective reduced masses. For example, going from $Cu^{37}Cl$ to $Cu^{35}Cl$, we observe a shift of 0.55 ± 0.2 cm^{-1} for TO(γ), much less than anticipated from the change in μ (~ 3.0 cm^{-1}). Therefore the TO(γ) peak cannot be attributed to a zinc-blende Γ-point phonon. On the contrary, its dependence on the isotopic composition is closer to that of a pure copper vibration, as can be seen when comparing it to the $1/\sqrt{m_{Cu}}$ dependence shown as the dashed line in Fig. 4. Moreover, the TO(γ) frequencies of samples with the same copper composition group together and only within these groups is the order as expected from the trends in their respective reduced masses.

It is also important to realize that the TO(γ) peak is a very narrow feature, having neither Gaussian nor Lorentzian line shape. Consequently, the experimental TO(γ) peaks of Fig. 3 are broadened by the spectrometer resolution and their line shape is distorted. Therefore, only spectra taken with the same slit width can be compared to each other. We have evaluated the width of TO(γ) in the observed spectra by fitting it to a Gaussian starting from the sharp rise on the lower-frequency side to higher values. Using several starting points for the fit we ensured that it does not critically affect the width. Subsequently we have corrected these values for the Gaussian resolution function of the spectrometer. The linewidths of TO(γ), $\Gamma_{TO(\gamma)}$, determined in this way are given in Table II.

The TO(β) peak also shifts as a result of isotope substitution. The detection of small changes in its Raman shift, however, is obscured by its considerable width and small intensity for some of the compounds. We have fitted spectra from several measurements in the range of 130–160 cm^{-1} with a Gaussian profile and plot the average TO(β) frequency over the reduced mass in Fig. 5. The TO(β) frequency for some of the compounds is also given in Table I. We would like to point out that there is no *a priori* reason to assume a reduced mass dependence, an issue which will be discussed below.

IV. INTERPRETATION

A. General features of the anharmonic decay

A number of publications deal with the broadening and energy shift of phonons due to their anharmonic decay.[39–44] Here we only summarize the main ideas and results. Most lattice dynamical calculations are performed in the *harmonic approximation*, where the crystal lattice potential is expanded to quadratic terms in the atomic displacements only. In a real crystal, however, the cubic and quartic terms in this expansion are often non-negligible. The coupling of the harmonic eigenstates due to such anharmonicities results in a shift and broadening of the normal modes. These are described by a complex phonon self-energy

$$\Sigma(\vec{q},j;\omega)=\Delta(\vec{q},j;\omega)+i\Gamma(\vec{q},j;\omega), \tag{1}$$

which depends on the frequency ω, phonon wave vector $\vec{q}$, and the branch j of the phonon. We consider the renormalization of zone center phonons ($\vec{q}=\vec{0}$) by anharmonic inter-

TABLE II. Measured and calculated values for the linewidth $\Gamma_{\mathrm{TO}(\gamma)}$ in $[\mathrm{cm}^{-1}]$ and the amplitude ratios of TO(γ) and TO(β). The measured values of $\Gamma_{\mathrm{TO}(\gamma)}$ are corrected for the spectrometer resolution. The trends in the linewidths and changes in the ratios of the amplitudes of TO(γ) and TO(β) are in good agreement with the Fermi resonance model. The errors are mean square deviations of several measurements.

Sample	$\Gamma_{\mathrm{TO}(\gamma)}$		$\frac{I(\mathrm{TO}(\gamma))}{I(\mathrm{TO}(\beta))}$	
	Measured	Calculated	Measured	Calculated
$^{63}Cu^{35}Cl$ [a]	0.9(1)	0.9	2.0(3)	2.1
$^{63}Cu^{nat}Cl$	0.74(9)	1.1	2.4(4)	1.6
$^{63}Cu^{37}Cl$	-	1.3	-	0.8
$^{nat}Cu^{35}Cl$	0.61(4)	0.6	2.84(05)	3.0
$^{nat}Cu^{nat}Cl$	0.75(4)	1.0	2.13(08)	1.9
$^{nat}Cu^{37}Cl$	0.92(6)	1.6	1.18(05)	1.0
$^{65}Cu^{35}Cl$ [a]	0.8(2)	0.4	3.5(3)	4.8
$^{65}Cu^{nat}Cl$	0.57(4)	0.6	3.1(2)	3.2
$^{65}Cu^{37}Cl$[b]	-	1.2	-	1.4

[a]Data were taken at $T=8$K; samples have different orientation and were grown by a different process (Ref. 36).

[b]The ^{37}Cl compound contains about 11% ^{35}Cl.

action. For small shifts Δ and broadenings Γ compared to the harmonic Raman frequency $\omega(\vec{0},j)$ the line shape of the Stokes Raman peak at low temperature ($kT \ll \hbar\omega$) is

$$I_S(\vec{0},j;\omega) \propto \frac{\Gamma(\vec{0},j;\omega)}{[\omega-\omega(\vec{0},j)-\Delta(\vec{0},j;\omega)]^2+\Gamma^2(\vec{0},j;\omega)}. \tag{2}$$

The broadening of the Raman line is then given by

$$\Gamma(\vec{0},j;\omega)=\frac{18\pi}{\hbar^2}\sum_{\vec{q},j_1,j_2}|V_3(\vec{0},j;\vec{q},j_1;-\vec{q},j_2)|^2[n(\vec{q},j_1)+n(-\vec{q},j_2)+1]\delta(\omega(\vec{q},j_1)+\omega(-\vec{q},j_2)-\omega). \tag{3}$$

$V_3(\vec{q},j;\vec{q}_1,j_1;\vec{q}_2,j_2)$ are the cubic coefficients in the expansion of the lattice potential in normal coordinates. In Eq. (3) we have already chosen the particular case in which a zone center phonon ($\vec{q}=\vec{0}$) with branch index j decays into two phonons with opposite wave vectors $\vec{q}_1=\vec{q},\vec{q}_2=-\vec{q}$ and branch indices j_1,j_2, respectively. The δ function in Eq. (3) ensures conservation of energy. At low temperature the thermal occupation number $n(\vec{q},j)$ vanishes. Therefore, if we assume constant matrix elements V_3, the right-hand side of Eq. (3) becomes proportional to the two-phonon density of states $\rho_2(\omega)$. Thus, a considerable broadening might be expected whenever the optical Raman frequency $\omega(\vec{0},j)$ coincides with a peak in the two-phonon density of states. However, this assumption may be an oversimplification, since V_3 also depends on the wave vector of the pair of phonons into which the mode decays.[43] This dependence is given by[39,42]

$$V_3(\vec{0},j;\vec{q},j_1;-\vec{q},j_2) = \frac{1}{6}\left(\frac{\hbar^3}{8N\omega(\vec{0},j)\omega(\vec{q},j_1)\omega(-\vec{q},j_2)}\right)^{1/2}\sum_{l',l''}\sum_{k,k',k''}\sum_{\alpha,\beta,\gamma}\times\Phi_{\alpha,\beta,\gamma}(0,k;l',k';l'',k'')\times\frac{e_\alpha(k|\vec{0},j)e_\beta(k'|\vec{q},j_1)e_\gamma(k''|-\vec{q},j_2)}{[M_kM_{k'}M_{k''}]^{1/2}}e^{i\vec{q}\cdot[\vec{R}(l')-\vec{R}(l'')]}, \tag{4}$$

where $\Phi_{\alpha,\beta,\gamma}$ is the third derivative of the interatomic potential with respect to displacements along the Cartesian coordinate axes α,β, and γ of the atoms $(0,k)$, (l',k'), and (l'',k''). The index l labels the primitive cell, while k denotes the two atoms within the primitive cell. The $\vec{e}(k|\vec{q},j)$ are the harmonic eigenvectors. M_k is the atomic mass and N the number of cells in the crystal. From the mass dependence of V_3 one can estimate the change of the decay rate with isotope substitution (see Sec. IV C).

The anharmonic shift Δ of a zone center optical phonon comprises contributions due to the thermal expansion of the lattice, a fourth-order phonon scattering term, and the third-order coupling just discussed. Since the first two effects result in an ω-independent shift, we only retain the third-order contribution.[26] Due to its frequency dependence, it can result in a line shape distortion [Eq. (2)]. As discussed before, it merely includes the decay of one phonon into two phonons of opposite wave vector; i.e., absorption of a phonon is excluded since these states are not occupied at low temperatures. Since Δ is the real part of the self-energy Σ [see Eq. (1)], it can be obtained from the imaginary part Γ through a Kramers-Kronig transformation.[44]

B. Calculation of model spectra

In this section we define a model which is solely based on third-order anharmonic interactions of lattice vibrations. It

allows us to calculate the Raman spectra of CuCl with different isotopic compositions. The only adjustable parameter is the third-order coupling constant V_3. Prevot *et al.* and Hennion *et al.* have measured the phonon dispersion of CuCl at low temperatures using inelastic neutron scattering.[23,24] We use the parameters which they obtained from fits of the 14-parameter shell model to their data and which are given in Ref. 24, to calculate the phonon dispersion of CuCl.[34,35] The phonon dispersion of CuCl is shown in Fig. 6 together with the two-phonon density of states $\rho_2(\omega)$. The optical phonon energies at the zone center scale with the reduced mass ($\sim 1/\sqrt{\mu}$), while the energies of the acoustic branches around the X and K points are determined by the copper vibrations ($\sim 1/\sqrt{m_{\mathrm{Cu}}}$), as indicated in Fig. 6(a). Patel and Sherman have investigated the $\vec{q}$ dependence of the eigenvectors of CuCl phonons using the rigid ion model as well as the shell model.[45] The eigenvector dispersions of the two models differ only slightly. The two-phonon density of states $\rho_2(\omega)$, shown in Fig. 6(b), is calculated by integrating over the irreducible wedge of the Brillouin zone using a mesh of 8240 points and an energy resolution of 0.1 cm^{-1}. In the energy region close to the harmonic TO frequency at the Γ-point [$\omega_{\mathrm{TO}}(\vec{0},j)=161.75\ \mathrm{cm}^{-1}$], the two-phonon density of states has peaks at 164 cm^{-1} and 169.5 cm^{-1}. These peaks are Van Hove singularities and arise from combinations of the LA and TA branches at the X and K points of the Brillouin zone (Fig. 6). However, the phonon frequencies determined in the neutron measurements are only accurate to within 6%. As a result, the exact location of the peaks in the two-phonon combination band is only known to within 12%. In order to avoid artifacts in the calculated spectra, we approximate $\rho_2(\omega)$, by connecting the peaks (X and K combinations) linearly and subsequently average it over a width of 1.5 cm^{-1}. We refer to the resulting quantity as $\overline{\rho_2}(\omega)$.

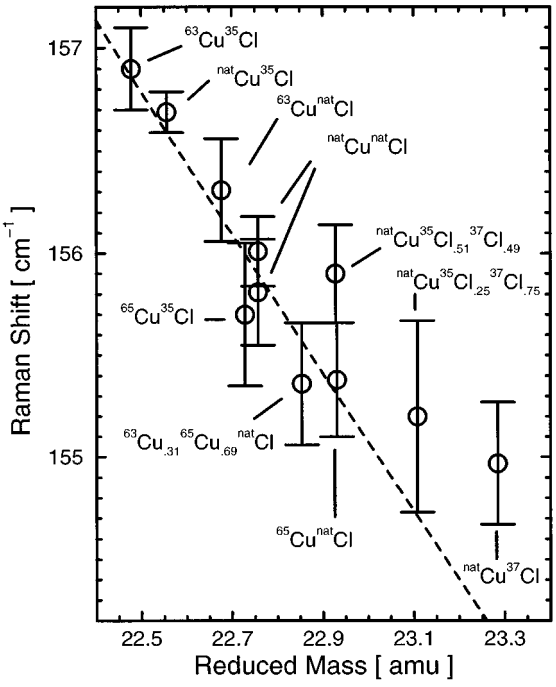

FIG. 5. Raman frequencies of the TO(β) peak versus the reduced mass ($T=2$ K, dashed line $\sim\mu^{-1/2}$).

The important feature in $\rho_2(\omega)$ is the sharp, precipitous drop at $\sim 170\ \mathrm{cm}^{-1}$, the highest energy TA+LA combination band. Its position and size are unaffected by the smoothing. This large drop results from the flatness of the TA branches in CuCl. The second approximation we make is that of a $\vec{q}$-independent matrix element V_3 in Eq. (3). The imaginary part of the phonon self-energy is then proportional to the two-phonon density of states: $\Gamma(\vec{0},j;\omega)=V_3^2\overline{\rho_2}(\omega)$.

Using these two approximations we can calculate the Raman spectrum of CuCl in the TO region. Performing a Kramers-Kronig transformation of $-\Gamma(\vec{0},j;\omega)$ we obtain the real part of the phonon self-energy $\Delta(\vec{0},j;\omega)$. Broadening Γ and shift Δ are shown in Fig. 7(a) as solid and dashed lines, respectively. We obtain the unrenormalized TO frequency $\omega_{\mathrm{TO}}(\vec{0},j)$ from the shell model, and show $\omega-\omega_{\mathrm{TO}}(\vec{0},j)$ as a straight dotted line in Fig. 7(a). For line broadenings Γ being either constant or small ($\Gamma\ll\Delta$) one expects, according to Eq. (2), an intense Raman signal when the first part in the denominator of the line shape function vanishes or goes through a minimum. This occurs when the straight line intersects or is very close to the real part of the self-energy Δ and, as a result, we find two peaks in the spectrum shown in Fig. 7(b). In order to obtain a good fit to the measured spectrum of ^{nat}Cu^{nat}Cl we have calculated model spectra for several coupling constants V_3. While larger V_3 increase the separation of TO(γ) from TO(β) they also increase the amplitude of TO(γ) with respect to that of TO(β). We have found $V_3^2=70\ \mathrm{cm}^{-2}$ to yield a good approximation to the observed line shape [Fig. 7(b)]. The frequency of the TO(γ) peak in the simulated spectrum is $\sim 3.8\ \mathrm{cm}^{-1}$ lower than the observed one.

At this point we want to discuss a principal problem of consistency in the outlined procedure: Inelastic neutron scattering, which was used to determine the phonon dispersion of CuCl, measures phonons which are already renormalized by the anharmonic interaction. Using these values to parametrize the harmonic shell model does not yield the unrenormalized harmonic frequencies.[24] However, in our calculation

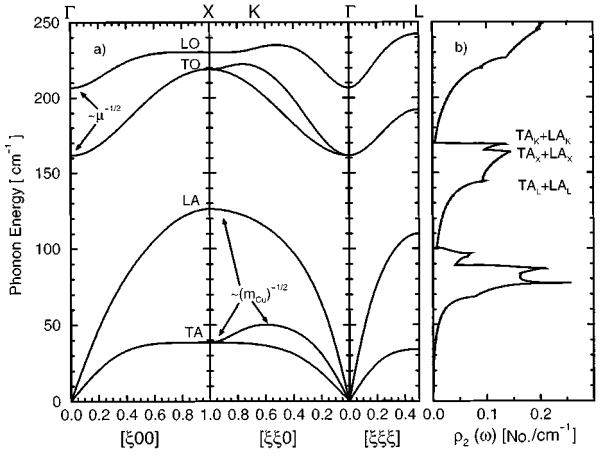

FIG. 6. (a) Phonon dispersion of natural CuCl along high-symmetry directions calculated using the shell model parameters given in Ref. 24. (b) Two-phonon density of states $\rho_2(\omega)$. The branch combinations which result in Van Hove singularities in the TO energy region are indicated.

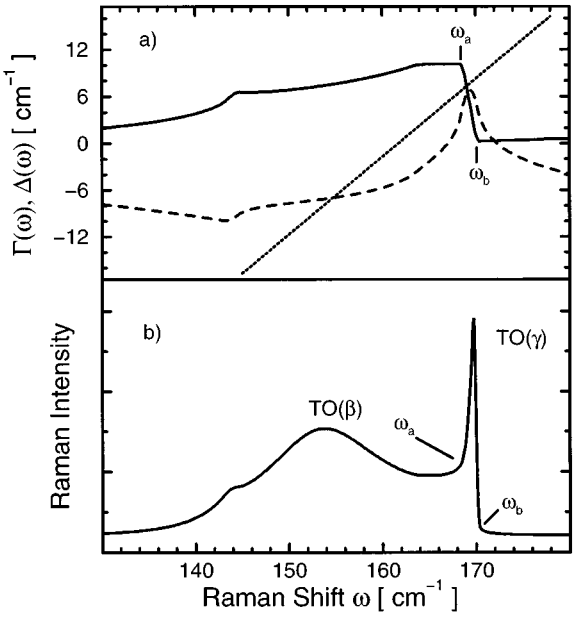

FIG. 7. Fermi resonance model of the TO anomaly in CuCl. (a) The solid line represents the imaginary part of the phonon self-energy $\Gamma(\omega)=V_3^2\overline{\rho_2}(\omega)$. The dashed line is the Kramers-Kronig related quantity $\Delta(\omega)$. The straight dotted line represents $[\omega-\omega_{\mathrm{TO}}(\vec{0},j)]$. (b) Spectrum of $^{\mathrm{nat}}\mathrm{Cu}^{\mathrm{nat}}\mathrm{Cl}$ simulated according to Eq. (2), using $V_3^2=70$ cm^{-2}; the intensity is given in arbitrary units.

of the complex self-energy $\Sigma(\vec{0},j;\omega)$ we implicitly used the phonon dispersion as if it were unrenormalized. A deviation of the *absolute* phonon frequencies calculated by applying the anharmonic renormalization from those being measured is therefore expected. Furthermore, we have neglected the thermal expansion and fourth-order contributions to the real part of the self-energy, which also result in a line shift and might account for the difference between the measurements and calculations. Even if the problem of renormalization were not to arise, neither the position of the drop in $\overline{\rho_2}(\omega)$ nor the harmonic frequency $\omega_{\mathrm{TO}}(\vec{0},j)$ would be known precisely. Both are inferred from a fit of the phonon dispersion to the shell model which does not necessarily reproduce the phonon frequencies with the same accuracy at all points in the Brillouin zone. Nevertheless, this problem of consistency has little effect on the *relative* shifts due to the isotope effect.

We have also omitted the effects of *isotope disorder* in our calculations; i.e., we treat the lattice dynamics in the framework of the virtual crystal approximation. The masses of the ions on the cation or anion sublattice are approximated by an average over the respective isotopic composition. Since the mass variance parameter g_μ in CuCl is reduced by about an order of magnitude as compared to germanium [Refs. 1 and 38(a)] or tin [Ref. 38(b)], where the observed disorder effects are already very small, isotope disorder induced shifts in the Raman spectra of CuCl should be negligible. The virtual crystal approximation is also justified by the good agreement of the measured LO(γ) frequencies with the expected reduced mass behavior for isotopically pure as well as isotopically disordered samples (Fig. 2). The linewidth of LO(γ), however, shows slight modifications with isotope disorder which are discussed at the end of Sec. IV C. The effect of isotope-disorder-induced scattering is even smaller for the TO zone center phonon, since the optical branches of the phonon dispersion bend monotonically upwards (Fig. 6). As a result there is only a negligible one-phonon density of states to scatter into and the resulting self-energy is strongly suppressed. Effects of *structural disorder* in which ions would be located on off-center sites were also omitted in our calculations. The relevance of this omission is discussed in Sec. IV D.

C. Discussion and comparison

In our calculation of the phonon dispersion of CuCl we only change the atomic masses M_k. The force constants of the shell model are assumed to remain unaffected by the isotope substitution. Calculating the two-phonon density of states $\rho_2(\omega)$ we obtain the line broadening $\Gamma(\vec{0},j;\omega)$ and the line shift $\Delta(\vec{0},j;\omega)$ for each isotopic composition, as outlined above. We calculate the Raman spectra for different isotopic compositions using the same anharmonic coupling constant $V_3^2=70$ cm^{-2} in all cases and the respective harmonic frequency $\omega_{\mathrm{TO}}(\vec{0},j)$. The resulting spectra are shown in Fig. 8. We observe that the TO(γ) frequencies for compounds with the same copper mass are similar. Within these groups TO(γ) shifts according to the trend expected from the reduced masses; i.e., the compound with the lighter chlorine isotope has a larger TO(γ) energy. The energies of TO(γ), shifted by $+3.8$ cm^{-1}, are also shown by the crosses in Fig. 4. We find an excellent agreement of our calculated isotope shifts with the observations.

The changes in phonon frequencies and eigenvectors due to isotope substitution lead to complex changes in the TO structure, which are automatically taken into account in our calculation. We can describe the results in simple terms: From Fig. 7 and the discussion in Sec. IV B, it is clear that the position of the TO(γ) phonon is mainly determined by the sharp drop in the imaginary part of the self-energy Γ. This drop stems from a Van Hove singularity of combinations of TA+LA acoustic bands around the *X* and *K* points. Since these modes involve mostly the copper ions, the drop shifts predominantly for Cu isotope substitution. To a first approximation, the drop in Γ does not shift with chlorine substitution, so that the TO(γ) peaks of compounds having the same copper mass form groups. Within these groups a second condition for the TO(γ) position is given by $\omega-\omega_{\mathrm{TO}}(\vec{0},j)=\Delta(\vec{0},j;\omega)$, or the point where the straight line in Fig. 7(a) is closest to the dashed line representing Δ. As we change the chlorine mass in compounds having the same copper mass, we shift the straight line in Fig. 7(a) by the full isotope effect on the reduced mass. Smaller chlorine masses shift the straight line to higher frequencies, and the point where it crosses or is closest to Δ shifts to higher frequencies as well. However, due to the nonvanishing slope of the real part of the self-energy Δ, the shift of this point is not as large as a reduced mass shift would imply.

The observed linewidths of the TO(γ) peak increase for the compounds made from natural copper, when the chlorine mass increases (see Table II). This is reproduced by our calculated spectra and can be visualized in Fig. 7 as follows:

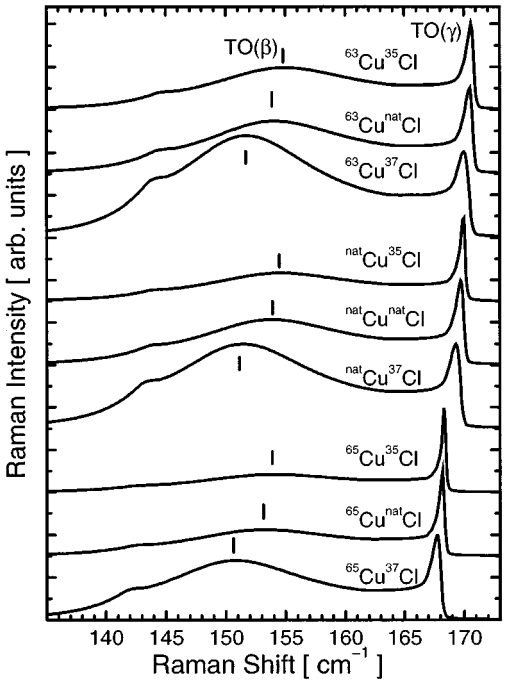

FIG. 8. Raman spectra calculated in the Fermi resonance scenario. The anomalous TO region is shown for CuCl of different isotopic composition ($T=0$ K, $V_3^2=70$ cm^{-2}). The slightly smaller actual mass of the ^{37}Cl compounds was not taken into account. The peak amplitudes are normalized with respect to TO(γ).

We define the frequencies ω_a and ω_b to denote the lower and upper edges of the drop in Γ. Leaving the copper mass unaltered these frequencies should remain constant due to the predominant copper character of the acoustic vibrations involved. The edges of $\overline{\rho_2}(\omega)$ at ω_a and ω_b are clearly reflected in the spectrum of Fig. 7(b). The linewidth $\Gamma_{\mathrm{TO}(\gamma)}$ then essentially depends on the amplitude of the spectrum between ω_a and ω_b. The maximum in the amplitude occurs for the smallest values of $[\omega-\omega_{\mathrm{TO}}(\vec{0},j)-\Delta(\vec{0},j;\omega)]$. Neglecting this value in comparison to Γ we find Eq. (2) to reduce to $I\sim\Gamma^{-1}$. Increasing the chlorine mass results in a shift of the dotted line in Fig. 7(a) towards lower frequencies. Consequently, Γ becomes larger. The amplitude of the resulting spectrum gets smaller, and the linewidth increases. A quantitative comparison of the calculated linewidths $\Gamma_{\mathrm{TO}(\gamma)}$ to the observed ones is obstructed by the finite spectrometer resolution. The smallest calculated linewidth is about 0.4 cm^{-1} and would be considerably broadened by the 0.45 cm^{-1} spectrometer resolution while the larger calculated linewidths of up to 1.6 cm^{-1} are largely unaffected. The linewidth $\Gamma_{\mathrm{TO}(\gamma)}$ also depends on intricate details of the two-phonon density of states between ω_a and ω_b. In view of these two points we still find a gratifying agreement between theory and experiment for the absolute values of $\Gamma_{\mathrm{TO}(\gamma)}$ as well as in the trends with isotope substitution.

Another rigorous test of the Fermi resonance model is to check whether it yields the correct trends for the relative amplitudes of TO(γ) and TO(β). As can be seen in Table II the experimental amplitude ratios are quite well reproduced by the theory. An exception is the ratio calculated for ^{65}Cu^{35}Cl which is predicted to be much larger than the measured one.

The calculated TO(β) frequencies, which are indicated by the vertical bars in Fig. 8, are about $\sim$2.2 cm^{-1} smaller than the measured ones (Table I). The changes of the frequencies with isotope substitution are, however, in good agreement with those shown in Fig. 5 and essentially proportional to the reduced mass. From Fig. 7 we notice that TO(β) peaks at the intersection of the dotted line $[\omega-\omega_{\mathrm{TO}}(\vec{0},j)]$ with the dashed line Δ. Shifts of the dotted line due to chlorine substitution result in a reduced mass type of behavior since the slope of Δ is small. Changing the copper mass results in a shift of both Δ and $\omega-\omega_{\mathrm{TO}}(\vec{0},j)$. The shift of the dotted line due to copper substitution does change the crossing point. Since Δ is flat, the crossing point is shifted just by the reduced mass effect on the dotted line. Due to its flatness, however, the shift of Δ does not move the point where the dotted and dashed lines intersect. We thus conclude that the shift of the TO(β) peak in CuCl should be reduced-mass-like, in good agreement with our data (Fig. 5).

In calculations which are similar to the procedure outlined for the TO structure we find a reduced mass behavior for LO(γ). The two-phonon density of states in the vicinity of the LO(γ) phonon is predominantly the combination of two LA modes near the L point. We approximate these by an average acoustic mode frequency of 105 cm^{-1}. The value of $(V_3^{\mathrm{TO}})^2=70$ cm^{-2} found above leads to an estimate of $(V_3^{\mathrm{LO}})^2=26$ cm^{-2}, taking only the frequency dependence of V_3 in Eq. (4) into account. Despite this being a rough approximation, we find linewidths of $\sim$1.6 cm^{-1}, which are in agreement with our observations (Table I).

The amplitude ratio $I(\mathrm{LO}(\gamma))/I(\mathrm{TO}(\gamma))$ of the simulation is up to a factor of 4 larger than the observed one, and the observed LO(γ) frequency is $\sim$6 cm^{-1} larger than calculated. With this approximate coupling constant we find that the changes of $(V_3^{\mathrm{LO}})^2$ due to isotope substitution are smaller than 5%. As a result the calculated linewidths vary by less than 0.08 cm^{-1}, a change much smaller than the observed differences in linewidths (see Table I). Thus we have to consider whether disorder-induced elastic scattering could give rise to the observed line broadenings: Despite their vanishing mass variance parameter g_μ, the compounds ^{63}Cu^{35}Cl and ^{65}Cu^{35}Cl have linewidths $\Gamma_{\mathrm{LO}(\gamma)}$ which are larger than those of the samples having no or small chlorine disorder (^{nat}Cu^{35}Cl, ^{nat}Cu^{37}Cl). However, these samples were produced in a different manner than the other compounds,[36] so that a poorer sample or surface quality may also be responsible for their larger linewidths. Furthermore, they were produced from a different ^{35}Cl batch, so that they might also contain different chemical impurities. Looking at the remaining samples which were produced using the same method (Table I) we realize that ^{nat}Cu^{35}Cl has the smallest disorder parameter g_μ as well as the smallest linewidth $\Gamma_{\mathrm{LO}(\gamma)}$. Going to ^{nat}Cu^{37}Cl the disorder parameter increases by about 12×10^{-5} together with an increase in the linewidth by about 0.14 cm^{-1}. The slightly larger disorder parameter of ^{nat}Cu^{37}Cl is due to the inclusion of ^{35}Cl (see Table I). The mass variance parameter g_μ of ^{63}Cu^{nat}Cl, ^{nat}Cu^{nat}Cl, and ^{65}Cu^{nat}Cl is similar and about 22×10^{-5} larger than that of ^{nat}Cu^{35}Cl. These compounds show comparable linewidths $\Gamma_{\mathrm{LO}(\gamma)}$ which are about 0.38 cm^{-1} larger than for ^{nat}Cu^{35}Cl. As a result we conclude that the differences in

linewidths are compatible with an isotope-disorder-induced broadening of the LO(γ) phonon. Further measurements on a very-high-resolution spectrometer are needed to clarify this point.

D. Off-center models

A number of models deal with off-center sites of copper ions in CuCl. The model as described by Vardeny and Brafman[28] and Livescu and Brafman[27] assumes that, in addition to the ideal sites in the lattice, the cations may occupy four equivalent off-center sites. These sites are supposed to be located along the [111] antibonding directions, i.e., towards the faces of the tetrahedron formed by the anions. The secondary minima of the potential are located within the anion tetrahedron. These authors suggest that the two inequivalent copper sites, together with the undisturbed anion lattice, give rise to two polar oscillators which can couple to light. They infer this conclusion in particular from polariton measurements, which they fit to two oscillators, i.e., four peaks LO(γ), TO(γ), LO(β), and TO(β). The LO(β) mode at $T=2$ K is reported to have a frequency of ~ 164 cm^{-1}. We would like to point out that it is very hard to discern a third peak around this frequency in the TO spectra of Fig. 3, which were taken with very high resolution. Nevertheless, the spectra in Fig. 3 show a weak shoulder between the TO(β) and TO(γ) peaks which is, however, well accounted for by the Fermi resonance model (Fig. 7). Also, in a polariton picture the LO(β) peak is not expected to move with the angle of incidence. The TO(γ) line, however, should change its position. The evidence for this behavior of TO(γ) in Fig. 1 of Ref. 28(c) is based on a rather weak feature. The much stronger main TO(γ) line, however, does not change its position at all. This is consistent with the acoustic phonon character of this line in the Fermi resonance picture. In order to obtain further insight it seems worthwhile to calculate the renormalization of the Fermi resonance in CuCl due to interaction with the photon field and to perform higher-resolution experiments.

A more quantitative description of this off-center model postulates the same mass dependence for both the TO(γ) and the TO(β) mode.[27] Since we have found a mass dependence of TO(γ) which is different from the one of TO(β), the off-center model in the form proposed in Ref. 27 clearly cannot account for the effects of isotope substitution on the Raman spectra.

Recent total energy calculations suggest that copper atoms on off-center sites form correlated defect clusters. Similar to the model of Livescu and Brafman,[27] these calculations find that the copper atoms are displaced along the [111] antibonding directions.[29,30] In contrast to the earlier model, however, the displacements are large, and the copper atoms tunnel through the face of the anion tetrahedron. Parks and Chadi[30] find that the formation of a cluster of four off-center copper atoms reduces the total energy of their supercell even further, as compared to the total energy of the same supercell comprising only one off-center copper atom. A local mode arising from these clusters would seem likely, but it is not clear whether this would involve mainly copper vibrations or correspond to a softened Cu-Cl mode. A local mode with predominant copper character[30] is ruled out by the reduced mass behavior of TO(β). When assigning TO(β) to a softened Cu-Cl vibration, we still have to account for TO(γ). In the framework of the off-center model, however, it must be the unrenormalized TO(Γ) phonon of the zinc-blende structure. Again this is excluded by the copperlike shift of TO(γ) with isotope substitution. As pointed out already in Ref. 32 our Raman measurements do not exclude the presence of structural disorder although they do not yield any evidence of it. However, the Fermi resonance model successfully predicts the observed shifts and intensity changes of the TO anomaly with isotopic substitution. It is therefore not necessary to invoke a second set of optical phonons.

Finally, we would like to mention two further first principles calculations on the bulk properties of CuCl. Kremer and Weyrich[46] reported full-potential linear muffin-tin orbital (LMTO) calculations of the TO frequencies at the Γ and X points for CuCl and other semiconductors. They find an unrenormalized TO frequency of 156 cm^{-1} and have also calculated the potential for displacement of Cu along the [111] direction. They do not find a secondary minimum which would indicate an off-center site for Cu in this compound. Wang *et al.*[47] have calculated the phonon dispersion in CuCl using a linearized augmented plane wave (LAPW) linear response method. Their value for $\omega_{\mathrm{TO}}(\vec{0},j)$ is 168.3 cm^{-1}. Therefore, both of these publications find unrenormalized zinc-blende TO frequencies which are between the observed TO(γ) and TO(β) peaks. In view of the inherent uncertainties of the calculations these values are in good agreement with the 161.8 cm^{-1} used as $\omega_{\mathrm{TO}}(\vec{0},j)$ in our model calculation.

First principles calculations of compounds in which the strongly localized d electrons take part in the binding are difficult. This is due to a large cutoff energy required for the plane-wave expansion of the localized d electrons. We believe that our data provide a basis for a stringent test of the quality of first principles calculations concerning the bulk properties of CuCl in particular and the treatment of d-electron levels close to the valence level in general. An attempt to calculate the TO phonon line shape in CuCl and its isotope effects from first principles thus seems worthwhile.

V. CONCLUSION

Several models have been proposed to explain the anomalous TO Raman spectrum of CuCl at low temperature: The Fermi resonance model by Krauzman *et al.*[21] which is supported by lattice dynamical calculations,[26] and various off-center models.[27–30]

We have investigated the Raman spectra of CuCl with different isotopic compositions at low temperature ($T=2$ K) and find good agreement with the Fermi resonance model. In this scheme anharmonic interactions, in which a zone center optic phonon decays into two acoustic phonons of opposite wave vector, renormalize the mode frequencies and alter the Raman line shape. In CuCl the unrenormalized TO zone center phonon interacts with a two-phonon combination band which is strongly peaked. Consequently, the TO phonon is

partly pushed out of the two-phonon continuum, which results in the TO(γ) peak. Its position is closely tied to the edge of the two-phonon density of states. Since this edge is due to Van Hove singularities, arising from the acoustic dispersion branches which involve mainly copper vibrations, it shows a copper-dominated isotope effect. For samples having the natural copper abundance the linewidth of the TO(γ) peak increases with the chlorine mass. The changes in the TO(β) frequency are reduced-mass-like, a fact which is also expected within the Fermi resonance model. For unaltered copper composition the ratio of the peak intensities of TO(γ) to TO(β) decreases with increasing chlorine mass. The unrenormalized LO phonon interacts with an almost flat two-phonon density of states. As a result it shifts according to the expected reduced mass behavior of a zone center phonon. The linewidth of LO(γ) comprises anharmonic as well as isotope-disorder-induced broadening. Using only one effective anharmonic coupling parameter V_3 we can account for all our experimental findings.

In contrast, off-center models do not account for the Raman data. The quantitative description of an earlier model[27] implies two reduced-mass-like oscillators which does not explain the different mass dependences of TO(γ) and TO(β). While we cannot exclude the existence of off-center defects in CuCl, they are neither necessary nor sufficient to explain the TO anomaly.

ACKNOWLEDGMENTS

A.G. gratefully acknowledges A. Debernardi for providing the code for the Brillouin zone integration and stimulating discussions. We thank V. Belitsky for a critical reading of the manuscript. Thanks are also due to M. Siemers and H. Hirt for their expert technical assistance and A. Schmeding for the analysis of the isotope concentration of $^{nat}Cu^{37}Cl$.

[1] M. Cardona, in *Festkörperprobleme/Advances in Solid State Physics*, Vol. 34, edited by R. Helbig (Vieweg, Braunschweig, 1994), p. 35.
[2] A. K. Ramdas, Solid State Commun. **96**, 111 (1995).
[3] E. E. Haller, J. Appl. Phys. **77**, 2857 (1995).
[4] T. Ruf, H. D. Fuchs, and M. Cardona, Phys. Bl. **52**, 1115 (1996).
[5] R. C. Buschert, A. E. Merlini, S. Pace, S. Rodriguez, and M. H. Grimsditch, Phys. Rev. B **38**, 5219 (1988).
[6] S. Zollner, M. Cardona, and S. Gopalan, Phys. Rev. B **45**, 3376 (1992).
[7] C. Parks, A. K. Ramdas, S. Rodriguez, K. M. Itoh, and E. E. Haller, Phys. Rev. B **49**, 14 244 (1994).
[8] N. Garro, A. Cantarero, M. Cardona, A. Göbel, T. Ruf, and K. Eberl, Phys. Rev. B **54**, 4732 (1996).
[9] A. Debernardi and M. Cardona, Phys. Rev. B **54**, 11 305 (1996).
[10] J. C. Phillips, Rev. Mod. Phys. **42**, 317 (1970).
[11] L. Pauling, Phys. Today **24** (2), 9 (1971).
[12] T. H. K. Barron, J. A. Birch, and G. K. White, J. Phys. C **10**, 1617 (1977).
[13] R. C. Hanson, K. Helliwell, and C. Schwab, Phys. Rev. B **9**, 2649 (1974).
[14] F. Raga, R. Kleim, A. Mysyrowicz, J. B. Grun, and S. Nikitine, J. Phys. (Paris) Colloq. **28**, C3-116 (1967).
[15] M. Cardona, Phys. Rev. **129**, 69 (1963).
[16] N. Garro, A. Cantarero, M. Cardona, T. Ruf, A. Göbel, C. T. Lin, K. Reimann, S. Rübenacke, and M. Steube, Solid State Commun. **98**, 27 (1996).
[17] T. Ruf *et al.*, in *The Physics of Semiconductors*, edited by M. Scheffler and R. Zimmermann (World Scientific, Singapore, 1996), p. 185.
[18] A. Göbel, T. Ruf, M. Cardona, C. T. Lin, J. Wrzesinski, M. Steube, K. Reimann, J.-C. Merle, and M. Joucla (unpublished).
[19] I. P. Kaminow and E. H. Turner, Phys. Rev. B **5**, 1564 (1972).
[20] T. Fukumoto, S. Nakashima, K. Tabuchi, and A. Mitsuishi, Phys. Status Solidi B **73**, 341 (1976).
[21] M. Krauzman, R. M. Pick, H. Poulet, G. Hamel, and B. Prevot, Phys. Rev. Lett. **33**, 528 (1974).
[22] M. L. Shand, H. D. Hochheimer, M. Krauzman, J. E. Potts, R. C. Hanson, and C. T. Walker, Phys. Rev. B **14**, 4637 (1976).
[23] B. Prevot, B. Hennion, and B. Dorner, J. Phys. C **10**, 3999 (1977).
[24] B. Hennion, B. Prevot, M. Krauzman, R. M. Pick, and B. Dorner, J. Phys. C **12**, 1609 (1979).
[25] J. Ruvalds and A. Zawadowski, Phys. Rev. B **2**, 1172 (1970).
[26] G. Kanellis, W. Kress, and H. Bilz, Phys. Rev. Lett. **56**, 938 (1986); Phys. Rev. B **33**, 8724 (1986); **33**, 8733 (1986).
[27] G. Livescu and O. Brafman, Phys. Rev. B **34**, 4255 (1986).
[28] Z. Vardeny and O. Brafman, (a) Phys. Rev. B **19**, 3276 (1979); (b) **19**, 3290 (1979); (c) **21**, 2585 (1980).
[29] Su-Huai Wei, S. B. Zhang, and Alex Zunger, Phys. Rev. Lett. **70**, 1639 (1993).
[30] C. H. Park and D. J. Chadi, Phys. Rev. Lett. **76**, 2314 (1996).
[31] A. Göbel, T. Ruf, M. Cardona, and C. T. Lin, Physica B **219&220**, 511 (1996).
[32] A. Göbel, T. Ruf, M. Cardona, C. T. Lin, and J. C. Merle, Phys. Rev. Lett. **77**, 2591 (1996).
[33] C. H. Park and D. J. Chadi, Phys. Rev. Lett. **77**, 2592 (1996).
[34] W. Cochran, Proc. R. Soc. London, Ser. A **253**, 260 (1959).
[35] K. Kunc and O. H. Nielsen, Comput. Phys. Commun. **17**, 413 (1979).
[36] C. T. Lin, E. Schönherr, A. Schmeding, T. Ruf, A. Göbel, and M. Cardona, J. Cryst. Growth **167**, 612 (1996).
[37] J. M. Zhang, T. Ruf, A. Göbel, A. Debernardi, R. Lauck, and M. Cardona, in *The Physics of Semiconductors*, edited by M. Scheffler and R. Zimmermann (World Scientific, Singapore, 1996), p. 201.
[38] (a) P. Etchegoin, H. D. Fuchs, J. Weber, M. Cardona, L. Pintschovius, N. Pyka, K. Itoh, and E. E. Haller, Phys. Rev. B **48**, 12 661 (1993); (b) D. T. Wang, A. Göbel, J. Zegenhagen, and M. Cardona, in *The Physics of Semiconductors*, edited by M. Scheffler and R. Zimmermann (World Scientific, Singapore, 1996), p. 197.
[39] J. Menéndez and M. Cardona, Phys. Rev. B **29**, 2051 (1984).
[40] R. A. Cowley, J. Phys. (France) **26**, 659 (1965).
[41] R. A. Cowley, Rep. Prog. Phys. **31**, 123 (1968).
[42] M. Balkanski, R. F. Wallis, and E. Haro, Phys. Rev. B **28**, 1928 (1983).

[43] E. Haro, M. Balkanski, R. F. Wallis, and K. H. Wanser, Phys. Rev. B **34**, 5358 (1986).
[44] A. A. Maradudin, A. E. Fein, and G. H. Vineyard, Phys. Status Solidi **2**, 1479 (1962).
[45] C. Patel and W. F. Sherman, Physica B **165&166**, 923 (1990).
[46] J. W. Kremer and K. H. Weyrich, Phys. Rev. B **40**, 9900 (1989).
[47] Cheng-Zhang Wang, R. Yu, and H. Krakauer, Phys. Rev. Lett. **72**, 368 (1994).